Supporting Information: Relevance of the drag force during controlled translocation of a DNA-protein complex through a glass nanocapillary

Roman D. Bulushev,[†] Sanjin Marion,[‡] and Aleksandra Radenovic[*,†]

†*Laboratory of Nanoscale Biology, Institute of Bioengineering, School of Engineering, EPFL, 1015 Lausanne, Switzerland*

‡*Institute of Physics, Bijenicka cesta 46, HR-10000 Zagreb, Croatia*

E-mail: aleksandra.radenovic@epfl.ch

S1   Materials and Methods

Quartz capillaries with a 0.3 mm inner diameter and a 0.4 mm outer diameter were purchased from Hilgenberg. They were pulled using the program HEAT = 620, FIL = 0, VEL = 30, DEL = 140, PUL = 150 on a laser-assisted pipette puller (P-2000, Sutter Instruments). A typical pulling time was 0.30 ± 0.03 sec and diameters of the pulled capillaries were in the range of $150 - 200$ nm. All pulled capillaries were shrunken under SEM Merlin (Zeiss) to sizes in the range of 20-120 nm according to Steinbock et al.[1]. Afterwards they were integrated in a PDMS sample cell and attached to a coverslip in a way that cis and trans chambers were connected only via the nanocapillary opening[2]. The sample cells with nanocapillaries were cleaned with oxygen plasma for 2-5 min at ≈ 50 W and filled with a buffer solution. Different

buffers used in this work are listed in Table S1. Air bubbles formed inside nanocapillaries were removed using a vacuum pump.

Table S1: Buffers used in experiments and corresponding conductance changes due to translocation of DNA-bound proteins.

Application	[KCl], mM	[Tris/HCl], mM	[Tris/ Boric acid], mM	[EDTA], mM	pH	Conductance change
Detection of DNA-EcoRI with nanocapillaries and optical tweezers	400	10	-	1	8.1	increase
	150	3	-	1	7.5	-
	40	-	3	1	8.7	-
Detection of DNA-RecA with nanocapillaries	1000	3	-	1	7.4	decrease
Detection of DNA-RecA with nanocapillaries and optical tweezers	1000	3	-	1	7.4	decrease
	150	3	-	1	7.2	decrease
	150	3	-	1	9.0	decrease
	150	10	-	-	8.0	decrease
	100	10	-	-	8.0	decrease
	40	3	-	-	8.0	decrease
Detection of DNA-RNAP with nanocapillaries and optical tweezers	40	3	-	1	8.1	decrease

To carry out modification of beads with DNA 3 μm polystyrene streptavidin-coated beads were incubated with biotinylated from one end λ-DNA (48.5 kb) or a DNA PCR fragment (9 kb). The ratio of beads to DNA was 1 to 500, the incubation buffer composed of 100 mM KCl, 10 mM Tris/HCl, pH 8.0. DNA constructs were obtained accordingly to Bulushev et al.[2] and Keyser[3]. To form DNA-protein complexes DNA-coated beads were further incubated with proteins.

DNA-RNAP complexes were obtained by incubating 60 pM of 9 kb DNA molecules with a biotin tag from one end and containing a promoter C of bacteriophage T7 with 20 nM of RNAP (Affymetrix) in the presence of 1 mM NTP (Thermo Scientific), except for UTP, in the buffer composed of 150 mM KCl, 10 mM MgCl$_2$, 40mM Tris/HCl, 1 mM DTT, 0.01% TritonX, pH 7.5 at 37°C, 90 min. In the absence of one NTP RNAP forms a paused transcription complex on a DNA promoter[4,5].

To form DNA-EcoRI complexes 50 pM of λ-DNA (New England BioLabs) was incubated

with 50 nM EcoRI (Invitrogen) in the buffer, containing 150 mM NaCl, 10 mM HEPES, 50 μM DTT, 1 mM EDTA, 100 μg/ml BSA at 30 °C, 30 min.

DNA-RecA complexes were formed by incubating 50 pM of λ-DNA with 100 nM-6.6 μM of RecA (New England BioLabs) and 85 μM-5.75 mM of ATPγS (Sigma-Aldrich) in the buffer containing 70 mM Tris/HCl, 10 mM MgCl$_2$, 5 mM DTT, pH 7.6 at 37 °C, 60 min. The ratio of DNA to RecA and ATPγS was adjusted depending on the required coverage of DNA molecules.

The setup combining optical tweezers and nanocapillaries described in details in Bulushev et al.[2]. For detection of DNA-RecA complexes a 1064 nm laser from Bulushev et al.[2] was displaced by a 830 nm 1 W Nd:YAG laser (Sacher Lasertechnik). Current and force signals were recorded using a custom-made LabVIEW program at the sampling frequency of 10 KHz. Calibration of optical tweezers was performed on 3 μm polystyrene beads using the power spectral density method[6]. The optical trap stiffness was set in the range of 30-80 pN/μm.

Translocation events of DNA-RecA complexes were recorded using an Axopatch 200B current amplifier (Molecular Devices) at 100 KHz in accordance with Steinbock et al.[7]. Prior to performing experiments, nucleoprotein complexes were purified from non-bound proteins using first gel filtration (Chroma Spin TE-1000) and afterwards centrifuged 2 times for 5 min at 10000 g using filters with molecular-weight cutoff 100 K (Pierce Concentrator, Thermo Scientific).

DNA-RecA samples for atomic force microscopy (AFM) were prepared using the protocol written above. The theoretical coverage ratio of λ-DNA was 100%. The concentration of the DNA deposited on the freshly cleaved mica was 1.25 ng/μl. The AFM images were acquired in air in tapping mode using an Asylum Research Cypher microscope. We used cantilevers (Olympus) with a spring constant of 1.7 N/m and a resonant frequency of 70 Hz.

S2 Stohastic model of DNA-pulling experiments

We followed a stochastic modelling scheme[8] as implemented by Spiering et al.[9] for nanopores and adapted it to the specifics of a nanocapillary. Used notations are shown in Fig. 1a. The model includes two state variables, the position of the bead r and the contour length of DNA outside the nanocapillary s. The state variables are part of a coupled set of Langevin equations with an external force determined by the total free energy $G(r, s)$. For the position of the bead r the temporal evolution is given by:

$$\eta_b \dot{r} = -\frac{\partial G(r, s)}{\partial r} + \sqrt{2k_B T \eta_b} g(t) \tag{S1}$$

and for the contour length of DNA s:

$$\eta_p \dot{s} = -\frac{\partial G(r, s)}{\partial s} + \sqrt{2k_B T \eta_p} g(t). \tag{S2}$$

Here $g(t)$ is a random time-dependent Gaussian δ-correlated noise of unity magnitude, $\eta_b = 5 \cdot 10^{-5} pNs/nm$ and $\eta_p = 1 \cdot 10^{-5} pNs/nm$ are values for the Stokes friction parameters for the bead and polymer, respectively. $k_B T \approx 25.7$ meV is the thermal energy at room temperature.

The total free energy $G(r, s)$ of the system consists of the electrostatic free energy of DNA $G_{DNA}(s)$, the elastic and entropic free energy for extending a DNA strand $G_{wlc}(r, s)$, the free energy coming from the harmonic optical trap $G_{ot}(r)$ and the free energy of a protein bound to the DNA strand $G_p(r, s)$:

$$G(r, s) = G_{DNA}(s) + G_{wlc}(r, s) + G_{ot}(r) + G_p(s) \tag{S3}$$

To determine the electrostatic contribution to the total free energy $G(r, s)$ we modelled the interior of the nanocapillary as two truncated cones[7]. The total potential then consists of the same functional dependance inside both parts with different characteristic lengths
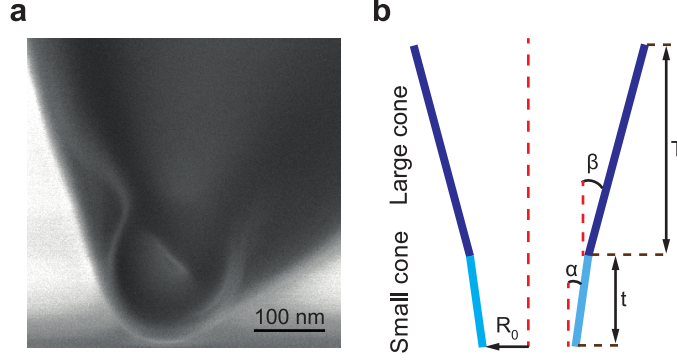
Figure S1: **SEM micrograph and sketch of a shrunken nanocapillary.** (a) Nanocapillary $\approx$ 23 nm in diameter shrunken under SEM. (b) We approximated the geometry of a shrunken nanocapillary with two truncated cones, where T and t – the taper lengths of large and small cones, respectively, β and α – the opening angles of large and small cones, respectively, R_0 – the radii of the opening.

and boundary conditions[2,10]. We defined t and T as the cone taper lengths, α and β - the opening angles, d and $D = d(1 + 2t \tan \alpha / d)$ - the smallest base diameter for the small and large cone, respectively (Fig. S1). The electrostatic potential $V(x)$ can be obtained from the continuity condition for the electric field and potential as:

$$V_1(x) = \Delta \Phi \frac{Ax}{(1 - \frac{x}{\xi})\xi} + \Delta \Phi \tag{S4}$$

in the small cone, and in the large cone as:

$$V_2(x) = \Delta \Phi \frac{B}{1 - \frac{x+t}{\zeta}} \tag{S5}$$

with two constants A and B expressed as:

$$A = \frac{(t + \xi)^2}{t^2 + t\xi + \zeta\xi} \tag{S6}$$

$$B = \frac{\zeta\xi}{t^2 + t\xi + \zeta\xi}. \tag{S7}$$

We have defined the constants $\xi = d/2 \tan \alpha$ and $\zeta = D/2 \tan \beta$ as the characteristic decay

lengths of the potential.

The DNA free energy is directly calculated from (S4) and (S5) by approximating that the DNA is a charged extended rod with the effective linear charge density λ, with a constant contribution coming from the DNA contour length s being on the energetically unfavourable side of the opening:

$$G_{DNA}(s) = \lambda \int V(x)\theta(-x)dx + \Delta\Phi\lambda s\theta(x) \qquad (S8)$$

where $\theta(x)$ - the Heaviside theta function. The first contribution comes into consideration when DNA is being pulled outside of the nanocapillary, giving a specific decay in the force profile[2]. The second contribution is the driving force on the DNA due to its negative charge. The effective linear charge density of the DNA λ includes both effects of counterion condensation and drag force from the electroosmotic flow[9,11,12].

Similarly to the DNA we obtained the free energy for a point-like charged protein at a position s_p along the DNA contour from the bead:

$$G_p(s) = \lambda \int V(x)q\delta(x - (s - sp))dx \qquad (S9)$$

here q is the effective charge of the protein with both electrostatic and electroosmotic flow contributions[9].

The elastic-entropic free energy G_{wlc} for extending a DNA strand[13]:

$$G_{wlc}(r, s) = \frac{k_B T}{L_p} \left\{ \frac{s}{4} \left[\frac{1}{1 - (r - \rho)/s} - 1 \right] - \frac{r - \rho}{4} + \frac{(r - \rho)^2}{2s} \right\} \qquad (S10)$$

here $L_p \approx 50$ nm is the persistence length of DNA, and $\rho = 1.5$ μm the size of the bead.

Additionally, we have the free energy from a harmonic pulling force of the optical trap:

$$G_{ot}(r) = \frac{1}{2}\kappa(z - r)^2 \qquad (S11)$$

where κ is the optical trap spring constant. The bead equilibrium position z was taken to

be a function of time $z = vt$, where $v \approx 500 \ nm/s$ was the experimental pulling speed.

The coupled set of equations (S1) and (S2) was solved in the time domain. Because of the linear relationship between the time and coordinate of the bead equilibrium position z all model force curves are shown as a function of z. The time step was $\Delta t \sim 10^{-5} s$ with additional refinements when the force terms $\partial G / \partial s$ and $\partial G / \partial r$ were larger than the contribution from thermal fluctuations. An example of such a solution is shown in Fig. S2 for a typical choice of parameters. Notice the change of the shape and mirroring of the force curves for oppositely charged proteins.
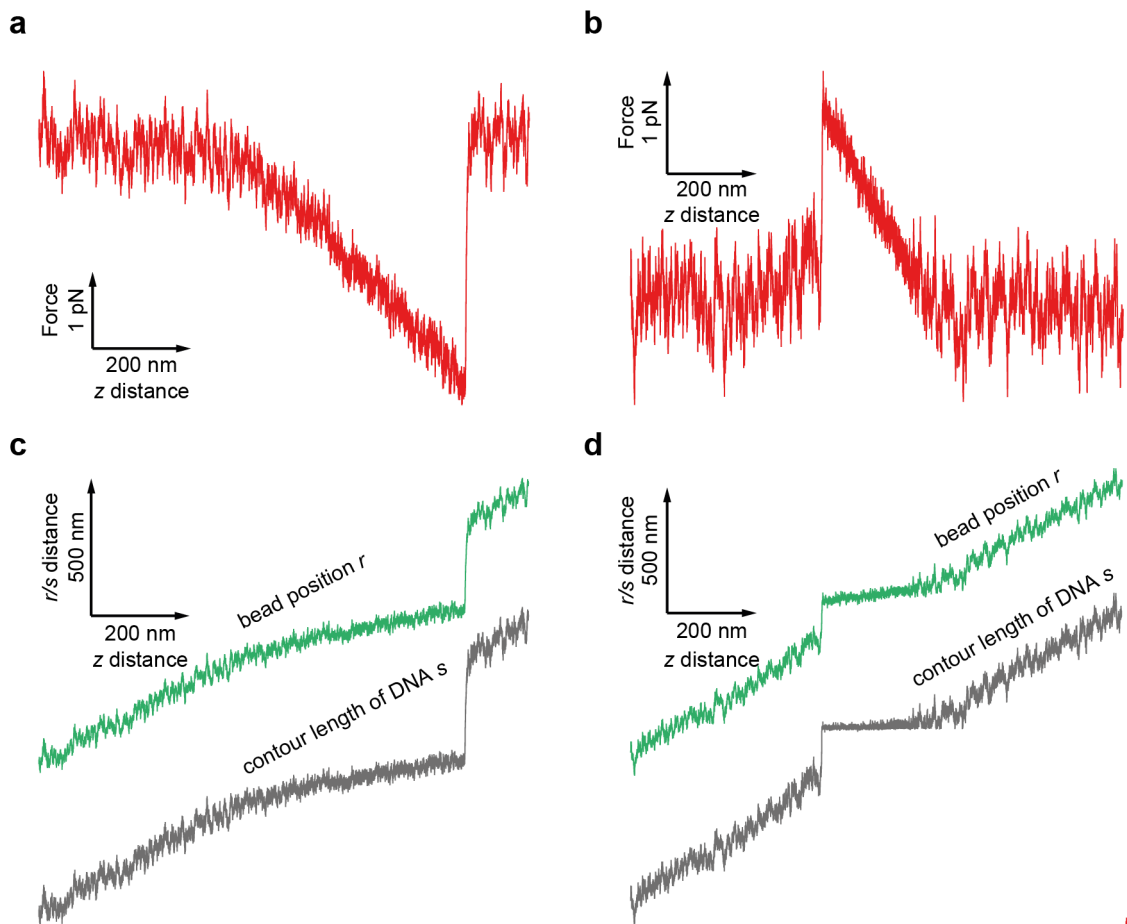

Figure S2: **Modelled force curves with corresponding state variable (s, r) curves for controlled translocation of negatively and positively charged DNA-protein complexes** . Force $F(z)$ (a) and lengths s and r (c) as a function of the bead equilibrium position z obtained using the stochastic model for parameters $\Delta\Phi = 100 \ mV$, $q = -30e$, $\xi = 100 \ nm$, $\zeta = 200 \ nm$, $s_p = 2500 \ nm$, $\kappa = 0.01 \ pN/nm$ and $\lambda = -0.1e/0.34 \ nm$. (b) and (d) were obtained at the same parameters except the sign of the protein charge was changed, *i.e.* $q = +30e$.

S3 COMSOL finite element model of a nanocapillary

A finite element method was implemented in an axially symmetric system in COMSOL multiphysics (version 4.4) represented by a quartz nanocapillary in a salt solution. The system was modelled as in Laohakunakorn $et\ al.$[14] using the Poisson-Nernst-Planck-Stokes equations. Electrostatic interactions between bound (quartz surface) and free charges (salt solution) were modelled using the Poisson equation for the electrostatic potential $\phi(\mathbf{r})$ as a function of the space coordinate $\mathbf{r}$:

$$\nabla^2 \phi(\mathbf{r}) = -\frac{\rho(\mathbf{r})}{\epsilon_0 \epsilon_r} \tag{S12}$$

with $\rho(\mathbf{r}) = e N_a \sum_i z_i c_i(\mathbf{r})$ - the density of free charge carriers, where z_i - the valency, $c_i(\mathbf{r})$ - the density in mol/m^3 of the ion i at a position $\mathbf{r}$, ϵ_0 - the vacuum permittivity, ϵ_r - the relative permittivity of the material (80 for water, 3.8 for quartz), N_a - the Avogadro constant and e - the elementary charge. The free charge densities $c_i(\mathbf{r})$ were subject to the Nernst-Planck equation for the ion flux $\mathbf{J}_i$ of species i with convection due to the fluid flow with a velocity $\mathbf{u}(\mathbf{r})$:

$$\mathbf{J}_i = -D_i \nabla c_i(\mathbf{r}) - \frac{D_i}{k_B T} z_i e c_i(\mathbf{r}) \nabla \phi(\mathbf{r}) + c_i(\mathbf{r}) \mathbf{u}(\mathbf{r}) \tag{S13}$$

where D_i are the diffusion coefficients of potassium and chloride ions ($D_1 = D_2 = 2 \cdot 10^{-9}\ m^2/s$).

The fluid flow was obtained using the Stokes equation with an electric body force $\rho(\mathbf{r})\nabla\phi(\mathbf{r})$ and pressure gradient ∇p:

$$\eta \nabla^2 \mathbf{u} = \rho(\mathbf{r}) \nabla \phi(\mathbf{r}) + \nabla p \tag{S14}$$

where η – the dynamic viscosity of water.

The mesh was constructed similar to previous works[14,15] using boundary layer refinement with minimal size at the boundaries of 0.1 nm and growth ratio of 1.2[14]. Near the nanocap-
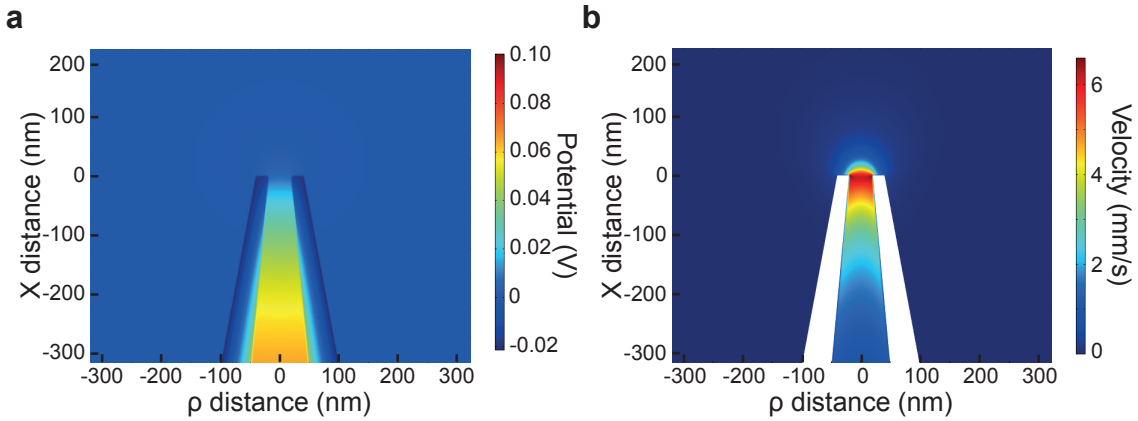
Figure S3: **Surface plots of the potential drop and electroosmotic flow velocity in a nanocapillary.** (a) Surface plot of the electrostatic potential near the nanocapillary tip. (b) Surface plot of the liquid flow velocity near the nanocapillary tip. Parameters used in the model were $\alpha = \beta = 5°$, $R_0 = 20$ nm, $c_0 = 150$ mM, $\Delta\Phi = 100$ mV, and the surface charge density of glass walls $\sigma = -20$ mC/m^2 .
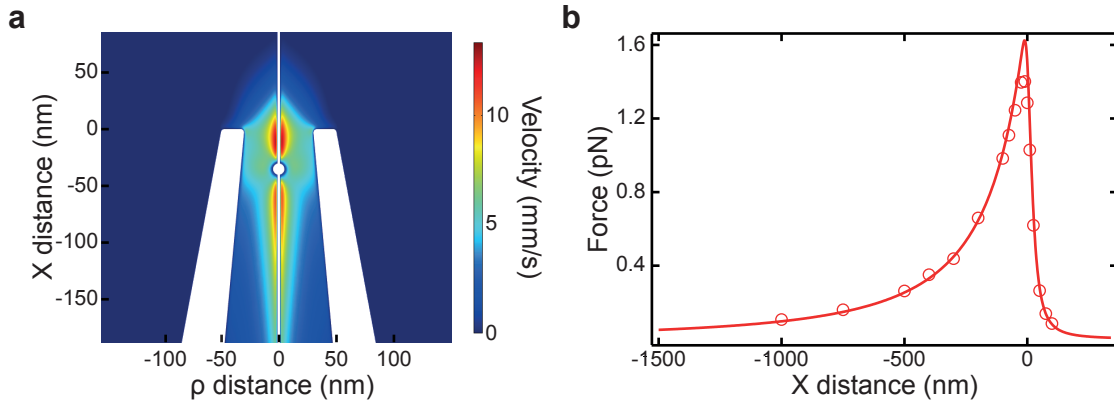

Figure S4: **Velocity flow profile and calculation of the drag force on a DNA-protein complex inside a nanocapillary** (a) Surface plot of a flow velocity $u(x)$ obtained with COMSOL inside a nanocapillary, containing a DNA-protein complex. DNA was modelled as a rod with the surface charge density $\sigma_{DNA} = -136.2$ mC/m^2 and the protein as a sphere with a radii $R_p = 5$ nm and surface charge density $\sigma_p = -25$ mC/m^2. All other parameters were kept the same as in Fig. S3. Comparison of the EOF-induced drag on a spherical DNA-protein complex (circles) and the Stokes drag $F_{drag} \sim R_p \eta u(x)$ obtained from Fig. S3b knowing the velocity profile $u(x)$ (line). The force calculated using a COMSOL built-in reaction on the protein and the Stokes drag force are related via a proportionality constant.

S9

illary opening the mesh was additionally refined until convergence was obtained. First we solved the Poisson-Nernst-Planck equations (without a flow) on a 1D domain, which was then mapped as the boundary condition for the general (3D) problem[14]. Fig. S3 shows surface plots of the electrostatic potential and electroosmotic flow profiles in a nanocapillary.

The drag force on a DNA-protein complex

In order to obtain the drag force on a DNA-protein complex we simulated a protein as a charged spherical object on a DNA strand. The calculated forces were obtained using a COMSOL built-in reaction force function for different distances x of the protein from the nanocapillary opening (circles in Fig. S4 b). This force was compared to the Stokes drag obtained from $F_{drag} \sim R_p \eta u(x)$ (line in Fig. S4 b), with $u(x)$ - the fluid velocity on the axis of symmetry without DNA or protein and R_p - the effective hydrodynamic radii of the protein . The Stokes drag was found to be a valid approximation with the only ambiguity of defining the proportionality constant. This constant depends on the choice of $u(x)$ and R_p.

Elongation of DNA inside nanocapillaries

Since for nanopores the electrostatic potential gradient is localised inside the pore it is reasonable to assume that DNA is extended for about a Kuhn length away from the opening[16]. In the case of nanocapillaries, the electric filed decays much slower than in nanopores as we go further inside the nanocapillary (Fig. S3a). To obtain the length of DNA that is extended inside the nanocapillary, we determined when the thermal (random) force $k_B T/L_p$ is stronger than the electrostatic force $E(x)L_p\lambda$ at the position x. Based on the calculated electric field $E(x)$ we obtained an estimate that the DNA is extended up to $20 - 30L_p$ inside the nanocapillary presented in Fig. S3.
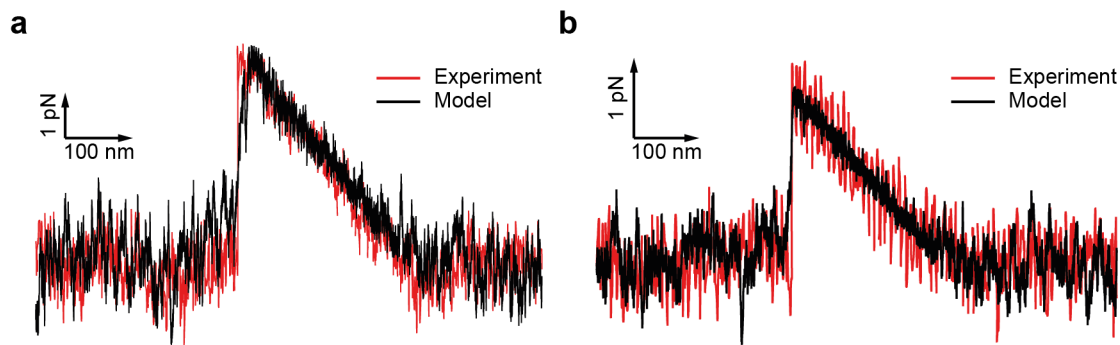
S4 Additional figures

Figure S5: **Force profiles of single DNA-EcoRI complexes**. Experimentally obtained results (red) and their fits to the stochastic model (black). (a) The data obtained in a 43 nm nanocapillary at 200 mV in 150 mM KCl, pH 7.5. (b) The data obtained in a 42 nm nanocapillary at 150 mV in 40 mM KCl, pH 8.7.
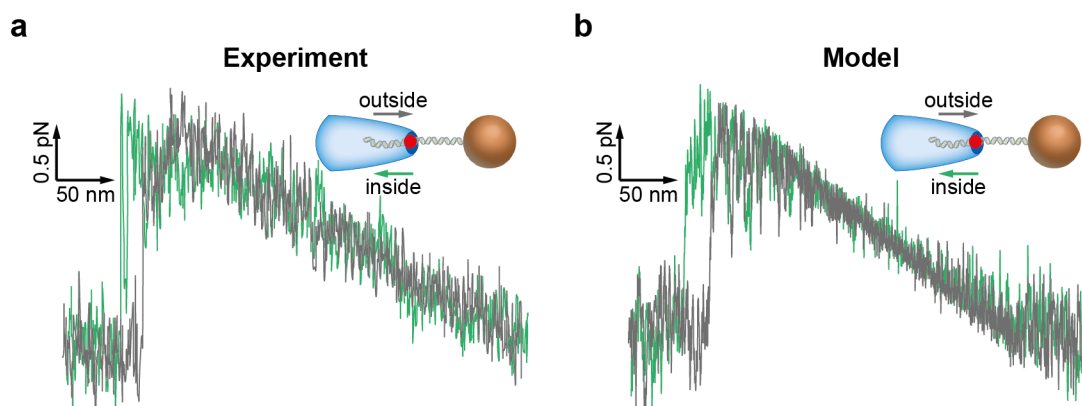

Figure S6: **Threading/unthreading of a DNA-EcoRI complex through a nanocapillary**. Experimentally (a) and theoretically (b) obtained force curves of a DNA-EcoRI complex pulled outside (grey curve) and inside (green curve) the nanocapillary opening. The experimental data were acquired in a 42 nm nanocapillary at 200 mV in 400 mM KCl, pH 8.1.
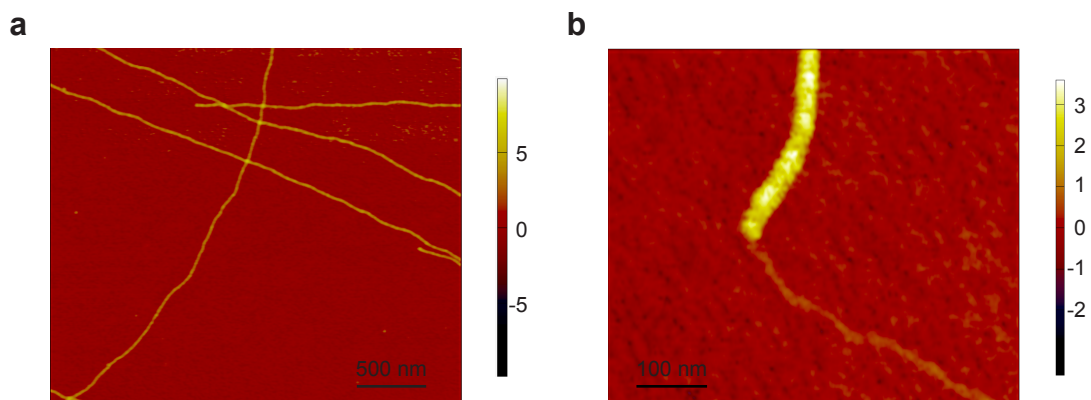
Figure S7: **AFM images of DNA-RecA complexes.** (a) DNA-RecA complexes form stiff filaments. (b) Even though the theoretical coverage of DNA molecules was 100% we found fragments of the DNA that did not form a complex with the protein. Relatively flexible ends of uncovered DNA could facilitate entrance inside nanocapillaries.
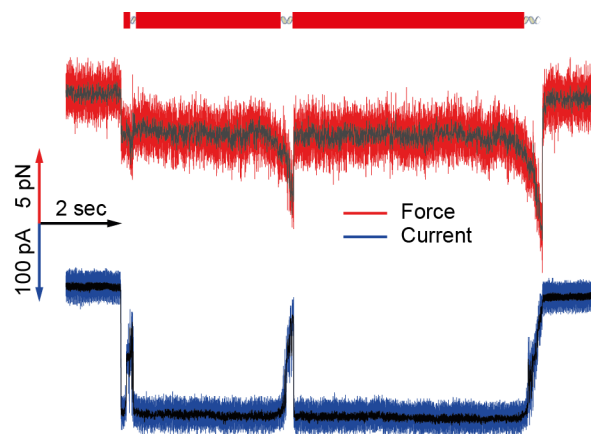
Figure S8: **Force and current profiles of a DNA-RecA complex in a nanocapillary with a small diameter.** Cartoon above represents coverage of the DNA with RecA (red rectangles). There are three parts of the DNA not completely covered with RecA. One can see additional details of the DNA-protein complex provided by the current signal. The data were acquired in a 21 nm nanocapillary at 150 mV in 150 mM KCl, pH 7.5. A nanopositioning stage was activated after entrance of the DNA with a velocity of 800 nm/s.
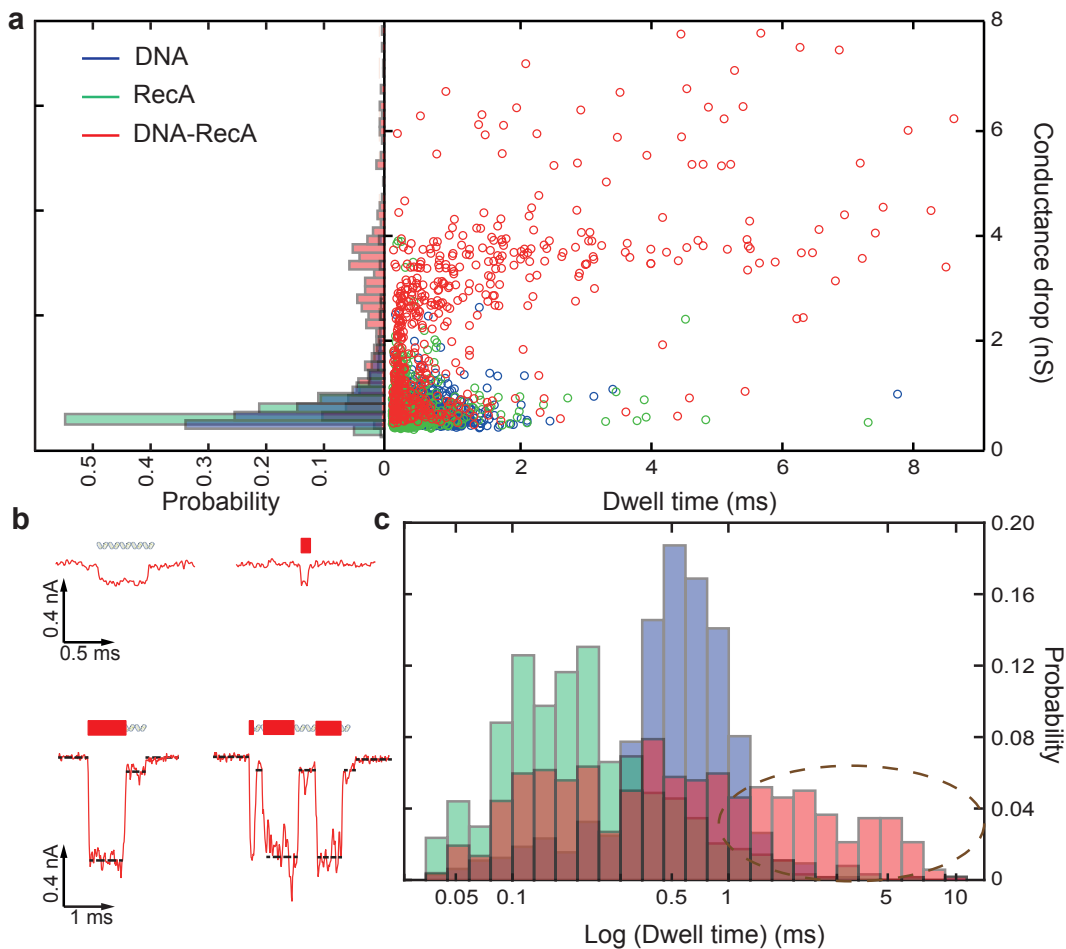
Figure S9: **Translocation of DNA partially coated with RecA in a glass nanocapillary.** (a) A scatter plot and conductance histogram recorded for λ-DNA, RecA and λ-DNA partially coated with RecA. We obtained 646 events for the DNA, 636 for RecA and 520 for DNA-RecA. Molecules were consequently translocated through the same glass nanocapillary and after recording of the data for each molecule the *cis* chamber was flushed with a buffer solution. The theoretical coverage of λ-DNA with RecA was $\approx 25\%$. Based on the conductance drops and dwell times we observed a mixture of RecA not bound to DNA, non modified DNA and DNA-RecA in the solution. RecA proteins and DNA were characterised by similar conductance drops, whereas a DNA-RecA complex had an additional peak with higher conductance drop. (b) Selected translocation events of λ-DNA, RecA and λ-DNA partially coated with RecA. Noteworthy, the presented time scale for DNA and RecA translocation events is twice shorter than for DNA-RecA. Conductance drops of DNA partially coated with RecA had two levels corresponding to the bare DNA and DNA-protein complex. (c) A dwell time histogram of the scatter plot in (a). In the case of DNA-RecA there were events corresponding to translocation of free RecA and DNA and events with longer dwell times (marked with a brown ellipse). High distribution of dwell times of DNA-RecA could be attributed to partially coating of the DNA with the protein. Lower electrophoretic force acting on the nucleoprotein filaments can be the reason of slower translocation of DNA-RecA than DNA, although we cannot exclude the possibility of its stronger interactions with glass walls. 1.5 times extension of partially coated λ-DNA could not result in the presence of events with much longer dwell times[17]. All data were acquired in a 35 nm glass nanocapillary at 250 mV in 1M KCl, pH 7.4.

References

(1) Steinbock, L. J.; Steinbock, J. F.; Radenovic, A. *Nano Lett.* **2013**, *13*, 1717–1723.

(2) Bulushev, R. D.; Steinbock, L. J.; Khlybov, S.; Steinbock, J. F.; Keyser, U. F.; Radenovic, A. *Nano Lett.* **2014**, *14*, 6606–6613.

(3) Keyser, U. F. *Methods Mol Biol* **2012**, *870*, 115–134.

(4) Levin, J. R.; Krummel, B.; Chamberlin, M. J. *J. Mol. Biol.* **1987**, *196*, 85–100.

(5) Severinov, K.; Goldfarb, A. *J. Biol. Chem.* **1994**, *269*, 31701–31705.

(6) Neuman, K. C.; Block, S. M. *Rev. Sci. Instrum.* **2004**, *75*, 2787.

(7) Steinbock, L. J.; Bulushev, R. D.; Krishnan, S.; Raillon, C.; Radenovic, A. *ACS Nano* **2013**, *7*, 11255–11262.

(8) Hummer, G.; Szabo, A. *Biophys. J.* **2003**, *85*, 5–15.

(9) Spiering, A.; Getfert, S.; Sischka, A.; Reimann, P.; Anselmetti, D. *Nano Lett.* **2011**, *11*, 2978–82.

(10) Ghosal, S. *Phys. Rev. E* **2006**, *74*, 041901.

(11) Ghosal, S. *Phys. Rev. E - Stat. Nonlinear, Soft Matter Phys.* **2007**, *76*, 1–3.

(12) van Dorp, S.; Keyser, U. F.; Dekker, N. H.; Dekker, C.; Lemay, S. G. *Nat. Phys.* **2009**, *5*, 347–351.

(13) Marko, J. F.; Siggia, E. D. *Macromolecules* **1995**, *28*, 8759–8770.

(14) Laohakunakorn, N.; Thacker, V. V.; Muthukumar, M.; Keyser, U. F. *Nano Lett.* **2015**, *15*, 695–702.

(15) Laohakunakorn, N.; Gollnick, B.; Moreno-Herrero, F.; Aarts, D. G. A. L.; Dullens, R. P. A.; Ghosal, S.; Keyser, U. F. *Nano Lett.* **2013**, *13*, 5141–5146.

(16) Lu, B.; Hoogerheide, D. P.; Zhao, Q.; Yu, D. *Phys. Rev. E* **2012**, *86*, 011921.

(17) Kowalczyk, S. W.; Hall, A. R.; Dekker, C. *Nano Lett.* **2010**, *10*, 324–328.